

Significance of Elastic Properties in Physics-Based Nonrigid Motion Modeling, A Numerical Sensitivity Analysis

Yong Zhang, Dmitry B. Goldgof and Sudeep Sarkar
Department of Computer Science & Engineering
University of South Florida
Tampa, FL 33620
(zhang, or goldgof, or sarkar)@csee.usf.edu

Abstract

Parameters used in the physical models for nonrigid motion simulation are often not known with high precision. It has been recognized that the commonly used assumptions about the parameters may have adverse effects on the modeling quality. We present an efficient sensitivity analysis method to assess the impact of those assumptions by examining the model's response to the parameter perturbation. Numerical experiments with both synthetic and real models show that (1) the normalized sensitivity distribution can help determine the relative importance of different parameters; (2) the dimensional sensitivity is useful in the assessment of a particular parameter assumption; (3) the model is more sensitive at the property discontinuity (heterogeneity). The proposed sensitivity analysis method is general and can also be applied to the assessment of other types of assumptions such as nonlinearity and anisotropy.

1 Introduction

Physics-based modeling has emerged as one of the most important techniques for nonrigid and articulated motion analysis. Its popularity is evidenced by the increasing number of publications each year as well as the diversity of the fields in which the papers appeared. For example, physical model has find applications in: nonrigid motion tracking [13, 10, 19], realistic animation and surgery simulation [11, 6], medical image registration [4, 20], cloud simulation [18], and shape representation and recognition [15], to name a few. More comprehensive survey and in-depth discussions on physics-based nonrigid motion analysis can be found in [1, 12].

In comparison to geometrical and mass-spring models, physical models based on continuum mechanics have relatively high computational complexity. Therefore, various assumptions are often made to simplify the model and its pa-

rameters. A commonly used assumption is that the material properties are isotropic and homogeneous. However, results from biomechanical tests [8] indicate that the mechanical behavior of many biological materials, especially soft tissues, can not be accurately described by such a simplified model. For example, muscles show strong anisotropic behavior and property heterogeneity in several orders of magnitude is common in human organs.

Recognizing the inadequacy of the simplified model, researchers start to investigate to what degree those assumptions may affect the model's performance by means of sensitivity analysis. Alterovitz *et al* [2] studied the effect of the physician-controlled and material parameters on the needle insertion simulation. Tanner *et al* [16] compared biomechanical models used for breast cancer diagnosis with different settings of boundary condition and material properties. However, those studies were done on the case-by-case basis using the *ad hoc* methods, and therefore the results and conclusions cannot be generalized to other applications. Moreover, the experiments were performed based on the assumption of homogeneous properties, which implies that the solution of a Dirichlet type problem could be independent of the property variation, and hence the subsequent sensitivity analysis could be invalid. Another limitation of their methods is that the sensitivity data is incapable of providing a complete picture of the model's spatial response to the parameter variation.

We propose a local gradient-based method that can be used to conduct a systematic and comprehensive sensitivity analysis of any physical model. Specifically, physics-based nonrigid motion modeling will benefit from such a sensitivity analysis in the following aspects: (1) the proposed method allows us to compare the relative importance of different parameters and quantify the impact of various assumptions on model's performance; (2) the algorithm is designed based on the adjoint state method, which significantly reduces the computational cost and is therefore suited for handling large scale finite element models; (3) the value of property parameters can be obtained by either the direct measurement [8] or the

indirect inference [14]. But those acquisition procedures are time-consuming and expensive. It would be economic to first conduct a sensitivity analysis to identify the primary parameters and then concentrate our effort on the acquisition of those parameters.

2 Sensitivity Analysis

Without losing generality, we discuss the deformation of a linear elastic body and its response to the parameter perturbation. However, the methodology developed here can be readily applied to the nonlinear systems. We will give a brief review of the primary problem [21, 8], and then discuss the sensitivity analysis method.

Primary Problem The deformation of an elastic body can be described by the following partial differential equations and boundary conditions (primary problem):

$$\rho \frac{\partial^2 u}{\partial t^2} = \nabla \cdot \sigma^T + B \quad (1)$$

$$\sigma = \lambda(\text{tr}\varepsilon)I + 2\mu\varepsilon \quad (2)$$

$$\varepsilon = \frac{1}{2}[\nabla u + (\nabla u)^T] \quad (3)$$

$$u = \bar{u}, \text{ on } \Gamma_1, \quad \frac{\partial u}{\partial n} = \bar{g}, \text{ on } \Gamma_2 \quad (4)$$

where u denotes the displacement vector, ρ is the mass density, t denotes time, σ is the stress tensor, T denotes transpose, B is the body force, $\nabla \cdot$ is the divergence operator with respect to a tensor, ε is the strain tensor, tr denotes trace, I is the identity matrix, λ and μ are the Lamé constants, ∇ is the gradient operator defined with respect to a vector, (\bar{u}, \bar{g}) are the Dirichlet and Neumann data on the boundary (Γ_1, Γ_2) , and n is the outward unit normal on the boundary.

(1), (2) and (3) are also known as the motion equation, the constitutive equation and the strain-displacement equation, respectively. Material properties such as the Young's modulus (E) and the Poisson's ratio (ν) are related to the Lamé constants by:

$$\mu = \frac{E}{2(1+\nu)}, \quad \lambda = \frac{\nu E}{(1+\nu)(1-2\nu)}$$

Using the Galerkin method, the primary problem in static equilibrium can be discretized into a linear finite element system:

$$Ku = b \quad (5)$$

where K is the stiffness matrix and b is the load vector.

For each finite element, an interpolation matrix (R_i) (the basis function) is used to relate the displacements in the local element coordinate (d_i) and the global coordinate (u):

$$d_i = R_i u \quad (6)$$

The corresponding constitutive equation (2) and strain-displacement equation (3) in discrete matrix form are:

$$\sigma_i = K_i \varepsilon_i \quad (7)$$

$$\varepsilon_i = D_i u \quad (8)$$

where K_i is the coefficient of stiffness matrix and D_i is a matrix derived from spatial differentiation of R_i . Note that K_i is comprised of material properties (E, ν).

With the above notations, the stiffness matrix and the load vector in (5) that assemble all elements become:

$$K = \sum_{i=1}^M \int_V D_i^T K_i D_i dV \quad (9)$$

$$b = \sum_{i=1}^M \int_V R_i^T q_{1i} dV + \sum_{i=1}^M \int_S R_i^T q_{2i} dS + \sum_{j=1}^L q_{3j} \quad (10)$$

where M is the total number of elements, V is the element size, q_{1i} is the body force within an element, q_{2i} is the surface traction, q_{3j} is point load, and L is the number of point loads.

Since we are interested in the sensitivity assessment of a system governed by (5) to the parameter variation, we rewrite (5) in terms of the parameter vector:

$$K(p)u = b(p) \quad (11)$$

where p denotes the generic parameter to be investigated, which could be material properties, stress or strain distribution, loading conditions, object's shape, and even the meshing scheme. Here we focus on the sensitivity analysis with respect to the Young's modulus and the Poisson's ratio: $p = \{p_j\} = \{E_j, \nu_j\}, j = 1, 2, \dots, M$.

Performance Measure and Dimensional Sensitivity The simplest sensitivity analysis method can be designed using a Taylor series that describes the relationship between the state variable (u) and the parameter (p):

$$\begin{aligned} u(p + \Delta p) &= u(p) + \sum_{j=1}^M \frac{\partial u}{\partial p_j} \Delta p_j + \\ &\frac{1}{2} \sum_{j=1}^M \sum_{l=1}^M \frac{\partial^2 u}{\partial p_j \partial p_l} \Delta p_j \Delta p_l + \dots \end{aligned}$$

where the first-order derivatives ($\frac{\partial u}{\partial p_j}$) are the coefficients of Jacobian matrix: $J = [\frac{\partial u_i}{\partial p_j}]$, ($i = 1, 2, \dots, N; j = 1, 2, \dots, M$), with N as the number of nodes in a finite element model.

The Jacobian matrix provides a local description of the response of state variable to the parameter change. However, for practical engineering problems, more sophisticated sensitivity analysis method is needed to help us understand how a given model depends on certain parameters, so that the most

significant one can be identified. To this end, a performance function (objective function) has to be defined:

$$H(u, p) = \int_{\Omega} f(u, p) d\Omega, \quad (12)$$

and the exact form of $f(u, p)$ is task-dependent.

We then define the *dimensional sensitivity* as:

$$S = \frac{dH(u, p)}{dp} = \int_{\Omega} \left[\frac{\partial f(u, p)}{\partial p} + \frac{\partial f(u, p)}{\partial u} \frac{du}{dp} \right] d\Omega \quad (13)$$

or in the discrete form:

$$S = [S_1, S_2, \dots, S_j, \dots, S_M] \quad (14)$$

$$S_j = \frac{dH(u, p)}{dp_j} = \frac{\partial H(u, p)}{\partial p_j} + \frac{\partial H(u, p)}{\partial u} \frac{du}{dp_j} \quad (15)$$

Without causing confusion, from now on, we will represent (14) and (15) with a single expression:

$$S = \frac{dH(u, p)}{dp} = \frac{\partial H(u, p)}{\partial p} + \frac{\partial H(u, p)}{\partial u} \frac{du}{dp} \quad (16)$$

Adjoint State Method The dimensional sensitivity can be computed by the finite difference approximation, the direct differentiation or the adjoint state method [5]. We use the adjoint state method because it is more efficient for large scale problems. For a finite element model of modest size, the number of elements could easily reach a couple of thousands, and the direct computation of sensitivity would be too costly.

The adjoint state method is based on the variational principle [9], and can be derived from the governing partial differential equations in the continuous space (1-4), or from the discrete system (11). We will follow the second route. We first differentiate (11) with respect to the parameter:

$$\frac{\partial K(p)}{\partial p} u + K(p) \frac{du}{dp} = \frac{\partial b(p)}{\partial p} \quad (17)$$

We then multiply (17) by an arbitrary vector ϕ (adjoint state variable):

$$\phi^T \frac{\partial K(p)}{\partial p} u + \phi^T K(p) \frac{du}{dp} = \phi^T \frac{\partial b(p)}{\partial p} \quad (18)$$

Combining (16) and (18), we have:

$$\begin{aligned} \frac{dH(u, p)}{dp} &= \frac{\partial H(u, p)}{\partial p} + \frac{\partial H(u, p)}{\partial u} \frac{du}{dp} \\ &\quad - \phi^T K(p) \frac{du}{dp} - \phi^T \frac{\partial K(p)}{\partial p} u + \phi^T \frac{\partial b(p)}{\partial p} \end{aligned} \quad (19)$$

Since ϕ is arbitrary, we chose a ϕ such that the following equation is satisfied (the second and third terms in the right side of (19)):

$$\frac{\partial H(u, p)}{\partial u} \frac{du}{dp} - \phi^T K(p) \frac{du}{dp} = 0 \quad (20)$$

(20) is equivalent to:

$$\left(\frac{du}{dp} \right)^T K^T(p) \phi = \left(\frac{du}{dp} \right)^T \left(\frac{\partial H(u, p)}{\partial u} \right)^T \quad (21)$$

which leads to the adjoint state equation:

$$K(p) \phi = \left(\frac{\partial H(u, p)}{\partial u} \right)^T \quad (22)$$

In the above derivation, we took advantage of the fact that the stiffness matrix is symmetric. Also note that the adjoint problem (22) is in the same form as the primary problem (11), except the load term, $\left(\frac{\partial H(u, p)}{\partial u} \right)^T$, which is also known as the pseudo-load.

Substituting (20) back into (19), we obtain:

$$\frac{dH(u, p)}{dp} = \frac{\partial H(u, p)}{\partial p} + \phi^T \left(\frac{\partial b(p)}{\partial p} - \frac{\partial K(p)}{\partial p} u \right) \quad (23)$$

As a result, we only need to solve the primary problem (11) and the adjoint problem (22) once, in order to obtain the state solution (u) and the adjoint state solution (ϕ), and then use (23) to compute the dimensional sensitivity. The adjoint state formulation can also be derived using the Lagrange multiplier method by treating (11) as the state equation, (12) as a constraint function and ϕ as the Lagrange multiplier [7].

Derivative Computation The partial derivative terms in (23) are needed to calculate the dimensional sensitivity. If the performance function is explicitly defined, we can directly compute the second term in (23) as:

$$\frac{\partial H(u, p)}{\partial p} = \int_{\Omega} \frac{\partial f(u, p)}{\partial p} d\Omega \quad (24)$$

In most applications, $f(u, p)$ is defined as a function of the state variable only, $f(u)$, and therefore its partial derivative with respect to the parameter becomes zero.

With the finite element formulation, the partial derivatives of the stiffness matrix and the load vector to the parameter can be expressed as:

$$\frac{\partial K(p)}{\partial p} = \sum_{i=1}^M \int_V D_i^T \frac{\partial K_i(p)}{\partial p} D_i dV \quad (25)$$

$$\begin{aligned} \frac{\partial b(p)}{\partial p} &= \sum_{i=1}^M \int_V R_i^T \frac{\partial q_{1i}(p)}{\partial p} dV + \\ &\quad \sum_{i=1}^M \int_S R_i^T \frac{\partial q_{2i}(p)}{\partial p} dS + \sum_{j=1}^L \frac{\partial q_{3j}(p)}{\partial p} \end{aligned} \quad (26)$$

Since we are interested in the sensitivity analysis with respect to the material properties only ($p = \{E, \nu\}$), the derivative terms in (25) and (26) only cause a slight increase of the computational cost.

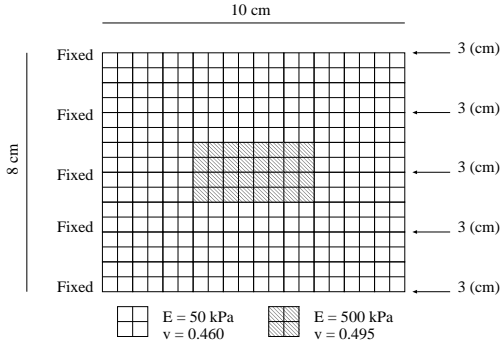


Figure 1. Model configuration.

Normalized Sensitivity Dimensional sensitivity as defined in (16) is suitable for studying the dependence of a model on a single parameter (note that the vector $p = [p_1, p_2, \dots, p_M]$ is viewed as a single parameter here). Because physical parameters usually have their own units, comparison among different parameters such as the Young's modulus and the Poisson's ratio using the dimensional sensitivity could be misleading. To remove the dimensional effect, we define the normalized sensitivity as:

$$S_n = \frac{p}{H(u, p)} \frac{dH(u, p)}{dp} = \frac{p}{H(u, p)} \left[\frac{\partial H(u, p)}{\partial p} + \frac{\partial H(u, p)}{\partial u} \frac{du}{dp} \right] \quad (27)$$

The normalized sensitivity measures the percentage change of the performance function to the percentage change of parameters. Therefore, it allows us to evaluate and rank the importance of different parameters with respect to their impact on the model on a common basis. The normalized sensitivity does not require changes of the computational procedure (adjoint state method) developed for the dimensional sensitivity. If statistical information about the measurement is available, a weighted normalized sensitivity function can also be considered.

3 Experiments With Synthetic Model

Model Configuration The model used in the experiments represents a 2D elastic object that has a size of $10 \times 8 \text{ (cm}^2\text{)}$. The object is discretized into a finite element mesh with 357 nodes and 320 elements (Figure 1). Elements are of quadrilateral thin shell type. All elements are assigned with isotropic properties ($E = 50 \text{ kPa}$, $\nu = 0.460$), except the 32 elements in the middle that have higher values ($E = 500 \text{ kPa}$, $\nu = 0.495$), which creates the property heterogeneity. This heterogeneous distribution is regarded as the true parameters: $p_t = \{E_t, \nu_t\}$. The Dirichlet boundary conditions are specified as follows:

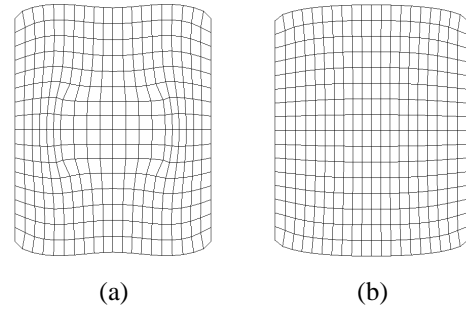


Figure 2. Deformed models using (a) the true heterogeneous properties and (b) the assumed homogeneous properties.

all nodes on the left side are fixed (displacement = 0 cm), while loads are exerted on the right side (displacement = 3 cm). The nodes on the top and bottom boundaries are set free.

With the true parameters and boundary conditions as specified above, the observation data (\bar{u}) is generated by running a forward simulation. The data vector is defined on all nodes ($\bar{u} = [\bar{u}_1, \bar{u}_2, \dots, \bar{u}_N]^T$). In real applications, the state variable may be measured only on parts of the object.

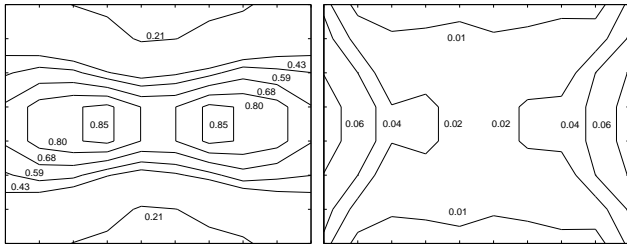
Performance Measure We define a performance function in the form of discrete Euclidean norm:

$$H(u) = \|f(u)\|^2 = \sum_{i=1}^N w_i^2 [u_i(p_a) - \bar{u}_i]^2 \quad (28)$$

where w_i is the weight coefficient assigned to the i th node, p_a denotes the assumed parameters, $u(p_a)$ is the solution using the assumed parameters and \bar{u} is the observation data generated with the true parameters. In all the experiments, we used the unit weight coefficient: $w_i = 1$.

This performance function consists of the state variable only. So the marginal sensitivity (the second term in (23)) becomes zero. In situations where the parameter measurements are available, they can be incorporated into the performance function ($H(u, p)$). If stress/strain analysis is of interest, they can also be included to construct a Neumann type performance function.

Since homogeneity is a commonly used assumption, we test a model that has the assumed homogeneous properties: $p_a = \{E_a = 50 \text{ kPa}, \nu_a = 0.460\}$. The deformed models with the true heterogeneous properties ($p_t = \{E_t, \nu_t\}$) and the assumed homogeneous properties ($p_a = \{E_a, \nu_a\}$) are shown in Figure 2. The discrepancy between the two deformed shapes is clearly visible. Next, we will demonstrate that (1) the normalized sensitivity can be used to identify the parameter that is most responsible for the discrepancy; (2) the



(a) S_n for Young's modulus (b) S_n for Poisson's ratio

Figure 3. Normalized sensitivity contours.

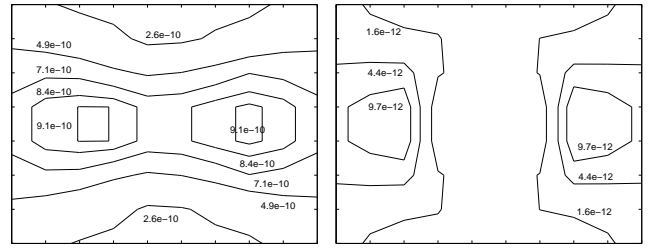
dimensional sensitivity is helpful for determining how good an assumption is.

Normalized Sensitivity Distribution The normalized sensitivities with respect to the Young's modulus and the Poisson's ratio are presented in Figure 3. The sensitivity distribution is plotted element by element as a contour map ($S_n = [S_{n1}, S_{n2}, \dots, S_{nM}]^T$). The sensitivity coefficient in an element (S_{nj}) represents the percentage change of the performance function due to a 1% change of the parameter value in that element. The difference between the two maps in terms of the magnitude of sensitivity coefficient suggests that the model is more sensitive to the Young's modulus than to the Poisson's ratio. In other words, with this particular model configuration, Young's modulus has a significant impact on the modeling accuracy, while the effect of the Poisson's ratio is secondary.

Further inspection of Figure 3 (a) reveals that the model is most sensitive at the property discontinuities. The geometry of the high sensitivity area matches the shape of heterogeneity. So, the sensitivity map is also informative about the location of parameter abnormalities to which effort should be dedicated to correct the original homogeneous assumption.

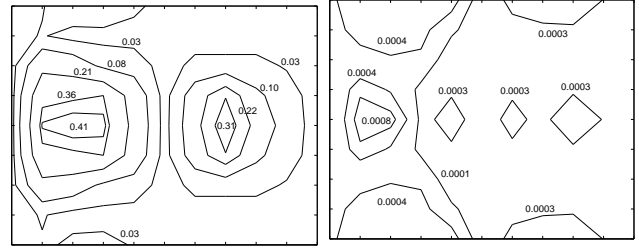
Dimensional Sensitivity Distribution It should be pointed out that certain formulations of the performance function may result in a sensitivity value of infinity. For example, with a performance function as defined in (28), the examination of (27) suggests that, as the assumed parameters approach the true parameters ($p_a \rightarrow p_t$), the normalized sensitivity goes to infinity ($S_n \rightarrow \infty$). Although it rarely occurs in real applications that our first assumption is as good as the true parameters, it is still wise to interpret the normalized sensitivity with cautions.

In the context of nonrigid motion modeling, we recommend a two-step sensitivity analysis procedure: (1) the normalized sensitivity can be used to quantify the relative importance of parameters in terms of their impact on the model's behavior; (2) once a parameter is considered as significant, the dimensional sensitivity can be used to assess the assump-



(a) S with $E_{hete} = 70$ kPa (b) S with $E_{hete} = 440$ kPa

Figure 4. Dimensional sensitivity contours.



(a) err with E_a and ν_t (b) err with E_t and ν_a

Figure 5. Relative error distributions

tions about the parameter. Without much loss of rigor, the closer the assumed parameters (p_a) are to the true parameters (p_t), the smaller the dimensional sensitivity is, and eventually it becomes zero everywhere when $p_a = p_t$.

We experimented with two assumptions about the Young's modulus inside the area of heterogeneity (the 32 elements in the center of the model): $E_1 = 70$ kPa and $E_2 = 440$ kPa. The Young's modulus in the background elements and the Poisson's ratio are the same as the true values. The dimensional sensitivity contours using those two assumptions are shown in Figure 4 (unit = $[m/Pa]$). The smaller magnitude of the second map indicates that the assumption ($E_2 = 440$ kPa) is much closer to the true value ($E_t = 500$ kPa) and is a better assumption than the first one ($E_1 = 70$ kPa). In the study of parameter estimation, the inverse algorithms also utilize the sensitivity information, although regularization is more important in solving the ill-posed inverse problems [20].

Relative Error Distribution The distribution of relative modeling error can also characterize the complex relationship between a model's behavior and its parameters. The relative modeling error is defined as follow:

$$err = \frac{|u(p_a) - \bar{u}|}{|\bar{u}|}. \quad (29)$$

To determine the contribution to the relative modeling error by an individual parameter, we carried out two experi-

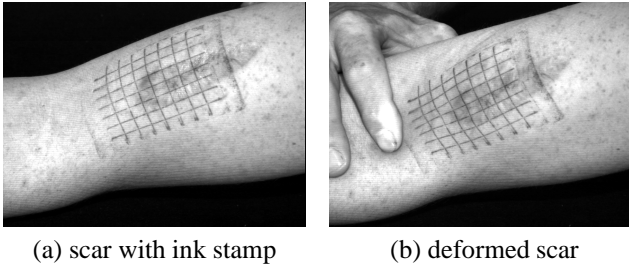


Figure 6. Deformation of burn scar.

ments, one with the true heterogeneous Young's modulus and the assumed homogeneous Poisson's ratio, and one with the assumed homogeneous Young's modulus and the true heterogeneous Poisson's ratio. The results are shown in Figure 5. The errors caused by an incorrect homogeneous assumption of the Young's modulus is around 10% to 40%, while the errors due to a bad assumption of the Poisson's ratio is less than 0.08%, which confirms the conclusion drawn from the sensitivity analysis that the Young's modulus is more significant than the Poisson's ratio under the configuration of this synthetic model.

4 Experiments With Burn Scars

The synthetic model described above has implications to many practical modeling problems, because the property values used are based on the published data. For example, in needle insertion simulation, a Young's modulus in the range of 40-160 kPa was used for prostate tissue [2]. In breast modeling, the variation of E among different tissues can be up to an order of magnitude, 10-88 kPa for the skin and 1-184 kPa for glandular tissue [3, 16]. The Poisson's ratio used in soft tissue modeling is often in the range of 0.465-0.495.

We applied the sensitivity analysis method to the burn scar assessment (see Figure 6). A finite element model was constructed using the rectangle grid of ink stamp (see [17] for detailed descriptions of the modeling procedure). Homogeneous properties were assumed ($E = 60$ kPa, $\nu = 0.495$). The normalized sensitivity contours are shown in Figure 7. Again, the scar model is more sensitive to the Young's modulus, although the difference between the sensitivity magnitude of E and ν is not as large as those observed in the synthetic model. As property heterogeneity, the Young's modulus of scar could be 2-10 times higher than that of normal skin (5-100 kPa). The similarity between the scar shape and sensitivity contours indicates that the model is more sensitive to the property heterogeneity. We then increased the Young's modulus of scar from 60 kPa to 450 kPa, and performed the dimensional sensitivity analysis (Figure 8). The smaller sensitivity coefficient of the second map (b) indicate that $E_{scar} = 450$ kPa is a better assumption.

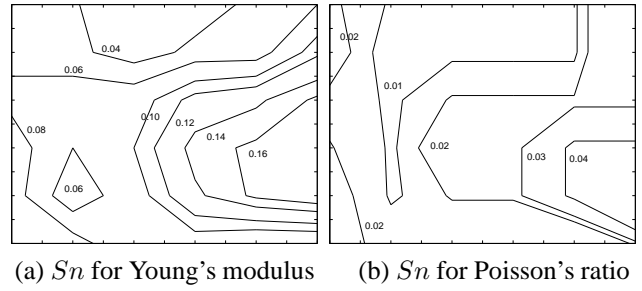


Figure 7. Normalized sensitivities of scars.

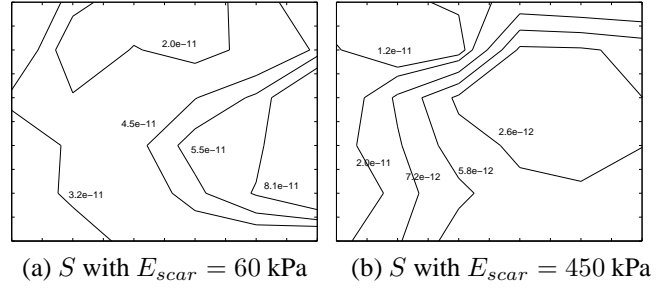


Figure 8. Dimensional sensitivities of scars.

5 Conclusions

The study of nonrigid motion using a physical model requires careful design and calibration of the model. Various assumptions about the model and its parameters must be thoroughly evaluated. We propose a sensitivity analysis method for quantitative and systematic diagnosis of the model's performance related to our assumptions about the parameters. The method is formulated using the first-order local gradient information. The adjoint state method is employed to reduce the computational cost of large scale models. A two-step procedure is recommended: (1) the normalized sensitivity is suited for identifying the most significant parameters; (2) the dimensional sensitivity can be used to assess the assumptions about a particular parameter.

Based on the two experiments, several observations can be made: (1) the model is more sensitive to the Young's modulus than to the Poisson's ratio; (2) the model is most sensitive at the property discontinuities (heterogeneity); (3) sensitivity map is informative about the location/geometry of the property abnormalities; (4) sensitivity analysis should not be confused with relative error analysis. The latter is often used for optimal shape design where the material properties are known *a priori* [9].

It should be stressed that the experiments reported here were performed with a linear model. The system response of a nonlinear model to the parameter variation is more complex. We will apply the proposed method to address the issues related to the nonlinear systems in future investigations.

Acknowledgments

This work was partially supported by the Grant CNS-0130768 from the National Science Foundation and the Moffitt Lee Cancer Research Center at University of South Florida.

References

- [1] J. K. Aggarwal, Q. Cai, W. Liao, and B. Sabata, "Nonrigid motion analysis: articulated and elastic motion," *Computer Vision and Image Understanding*, 70(2), pp. 142-156, 1998.
- [2] R. Alterovitz, K. Goldberg, J. Pouliot, R. Taschereau, and I-Chow Hsu, "Needle insertion and radioactive seed implantation in human tissues: simulation and sensitivity analysis," *Proc. of the 2003 IEEE Inter. Conf. on Robotics and Automation*, pp. 1793-1799, 2003.
- [3] F. S. Azar, D. N. Metaxas, and M. D. Schnall, "Methods for modeling and predicting mechanical deformations of the breast under external perturbations," *Medical Image Analysis*, vol. 6, pp. 1-27, 2002.
- [4] R. Bajcsy, and S. Kovacic, "Multiresolution elastic matching," *Computer Vision, Graph. and Image Proc.*, vol. 46, pp. 1-21, 1989.
- [5] D. G. Cacuci, *Sensitivity and Uncertainty Analysis: Theory (Volume I)*, A CRC Press, 2003.
- [6] S. Cotin, H. Delingette, and N. Ayache, "Real-time elastic deformations of soft tissues for surgery simulation," *IEEE Trans. on Visualization and Computer Graphics*, vol. 5, no. 1, pp. 62-73, 1999.
- [7] K. Dems and Z. Mroz, "Variational approach to sensitivity analysis in thermo-elasticity," *J. Thermal Stresses*, (10), pp. 283-306, 1987.
- [8] Y. C. Fung, *Biomechanics; Mechanical Properties of Living Tissues*, Springer-Verlag, 2nd ed. 1993.
- [9] E. J. Haug, K. K. Choi, and V. Komkov, *Design Sensitivity Analysis of Structural Systems*, Academic Press, 1986.
- [10] W. C. Huang, and D. B. Goldgof, "Nonrigid motion analysis using nonlinear finite element modeling," *SPIE Geometric methods in Computer Vision II*, SPIE(2031), pp. 404-414, 1993.
- [11] Y. Lee, D. Terzopoulos, K. Waters, "Realistic modeling for facial animation," *SIGGRAPH*, Los Angeles, CA, August, pp. 55-62, 1995.
- [12] D. Metaxas, *Physics-based Deformable Models: Applications to Computer Vision, Graphics and Medical Imaging*, Kluwer Academic Publishers, 1997.
- [13] D. Metaxas, and D. Terzopoulos, "Shape and nonrigid motion estimation through physics-based synthesis," *IEEE PAMI*, vol. 15, no. 6, pp. 580-591, 1993.
- [14] R. Muthupillai, D. J. Lomas, P. J. Rossman, J. F. Greenleaf, A. Manduca, and R. L. Ehman, "Magnetic resonance elastography by direct visualization of propagating acoustic strain waves," *Science*, vol. 269, pp. 1854-1857, 1995.
- [15] A. Pentland, and S. Sclaroff, "Closed-form solutions for physically based shape modeling and recognition," *IEEE PAMI*, vol. 13, no. 7, pp. 715-729, 1991.
- [16] C. Tanner, A. Degenhard, J. Schnabel, C. Hayes, L. I. Sonoda, M. O. Leach, R. Hose, D. L. G. Hill, and D. J. Hawkes, "A method for the comparison of biomechanical breast models," *Proc. of Workshop on Math. Methods in Biomed. Image Anal.*, Hawaii, pp. 11-18, 2001.
- [17] L. V. Tsap, D. B. Goldgof, S. Sarkar, and P. S. Powers, "A vision-based technique for objective assessment of burn scars," *IEEE Trans. Med. Imag.*, vol. 17, no. 4, pp. 620-633, 1998.
- [18] L. Zhou, C. Kambhamettu, D. B. Goldgof, K. Palaniappan, and F. Hasler, "Tracking nonrigid motion and structure from 2D satellite cloud images without correspondences," *IEEE Trans. on Pattern Analysis and Machine Intell.*, vol. 23, no. 11, pp. 1330-1336, 2001.
- [19] Y. Zhang, D. B. Goldgof, S. Sarkar, and L. Tsap, "Tracking objects using recovered physical motion parameters," *Proc. of 16th Inter. Conf. on Pattern Recognition (ICPR)*, pp. 10-13, Canada, 2002.
- [20] Y. Zhang, D. B. Goldgof, S. Sarkar, "Towards physically-sound registration using object-specific properties for regularization," *2nd Inter. Workshop on Biomed. Image Registration*, pp. 358-366, 2003.
- [21] O. C. Zienkiewicz, *The Finite Element Method*, 3rd edition, McGraw-Hill, 1977.